Indium nitride: a narrow gap semiconductor

J Wu

Applied Science and Technology Graduate Group, University of California, Berkeley and Materials Sciences Division, Lawrence Berkeley National Laboratory, Berkeley, CA 94720

W Walukiewicz, K M Yu, J W Ager III

Materials Sciences Division, Lawrence Berkeley National Laboratory, Berkeley, CA 94720

E E Haller

Department of Materials Science and Engineering, University of California, Berkeley and Materials Sciences Division, Lawrence Berkeley National Laboratory, Berkeley, CA 94720

Hai Lu, William J Schaff

Department of Electrical and Computer Engineering, Cornell University, Ithaca, NY 14853

Abstract. The optical properties of wurtzite InN grown on sapphire substrates by molecular-beam epitaxy have been characterized by optical absorption, photoluminescence, and photomodulated reflectance techniques. All these three characterization techniques show an energy gap for InN between 0.7 and 0.8 eV, much lower than the commonly accepted value of 1.9 eV. The photoluminescence peak energy is found to be sensitive to the free electron concentration of the sample. The peak energy exhibits a very weak hydrostatic pressure dependence and a small, anomalous blueshift with increasing temperature. The bandgap energies of In-rich InGaN alloys were found to be consistent with the narrow gap of InN. The bandgap bowing parameter was determined to be 1.43 eV in InGaN.

1. Introduction

Group III-nitrides are now a widely studied class of semiconductor materials. Both GaN and $In_xGa_{1-x}N$ with small x are very efficient light emitters, even in samples with relatively high densities of structural defects, and are used as component layers in a wide range of opto-electronic devices [1]. In contrast, InN has been observed to date to be a very poor light emitter. Results of early studies of the interband optical absorption performed on InN thin films deposited by sputtering techniques [2,3] and metalorganic

vapor phase epitaxy [4] were interpreted as being consistent with a fundamental energy gap of about 2 eV. However, despite extensive efforts, no light emission associated with the energy gap near 2 eV has ever been reported in these early studies of InN.

Recent improvements in epitaxial growth techniques have led to the availability of InN films with considerably lower electron concentrations and much higher electron mobilities. Electron concentrations in the mid 10^{18} cm^{-3} with room temperature electron mobilities well in excess of 1000 cm^2/Vs have been achieved by these methods [5-7]. It has been reported most recently that those improved InN films show a strong photoluminescence at energies around 1 eV [7]. Since it has been also found that the position of the photoluminescence energy correlates with the onset of strong absorption, it has been argued that the optical transition at about 1 eV corresponds to the fundamental bandgap of InN [7].

In this paper we report comprehensive studies of the optical properties of InN and InGaN samples. Our optical absorption, photomodulated reflection, and hydrostatic pressure and temperature dependent photoluminescence results are consistent with an intrinsic fundamental bandgap of InN between 0.7 and 0.8 eV. We have also found that the low energy gap exhibits unusual temperature and pressure dependencies. The bandgaps of In-rich InGaN alloys were also measured and found to be consistent with the narrow bandgap of InN.

2. Experimental

InN and $In_{1-x}Ga_xN$ films were grown on (0001) sapphire with an AlN buffer layer by molecular-beam epitaxy [8]. The thickness of the buffer layer ranges from 70 nm to 200 nm. The film thickness is between 120 nm to 1000 nm. The details of the growth process have been published elsewhere [8]. X-ray diffraction studies have shown that high-quality wurtzite-structured epitaxial layers formed with their c-axis perpendicular to the substrate surface. For $In_{1-x}Ga_xN$ films the Ga atomic fraction was determined by x-ray diffraction assuming complete lattice relaxation.

The samples were characterized by conventional optical absorption (abs), photoluminescence (PL) and photomodulated reflectance (PR) spectroscopies. The optical absorption measurements were performed on a CARY-2390 NIR-VIS-UV spectrophotometer. The PL signals were generated in the backscattering geometry by excitation with the 515 nm line of an argon laser. The signals were then dispersed by a SPEX 1680B monochromator and detected by a liquid-nitrogen cooled Ge photodiode. For the pressure-dependent PL studies, the sapphire substrates were thinned down to ~ 20 μm, and the samples were cut into small chips ~100×100 μm^2 in size and mounted into a gasketed diamond anvil cells for the application of hydrostatic pressure. For the PR experiments, quasi-monochromatic light from a halogen tungsten lamp dispersed by a 0.5m monochromator was focused on the sample as a probe beam (~1mm beam size). A chopped HeCd laser beam (442 nm) provided the modulation.

3. Band gap of InN

Figure 1 shows the optical characteristics of a typical InN sample. The free electron concentration in this sample was measured by Hall Effect to be 5×10^{18} cm^{-3}. The optical absorption curve shows an onset at ~0.78 eV. The absorption coefficient increases gradually with increasing photon energy and reaches a value of more than 10^4 cm^{-1} at the photon energy of 1 eV. This high value of the absorption coefficient is typical for interband absorption in semiconductors [9]. It is important to emphasize that there is no noticeable change in the absorption in the 1.9 to 2.0 eV region, *i. e.*, in the energy range of previously reported bandgaps in InN [3, 4, 10].

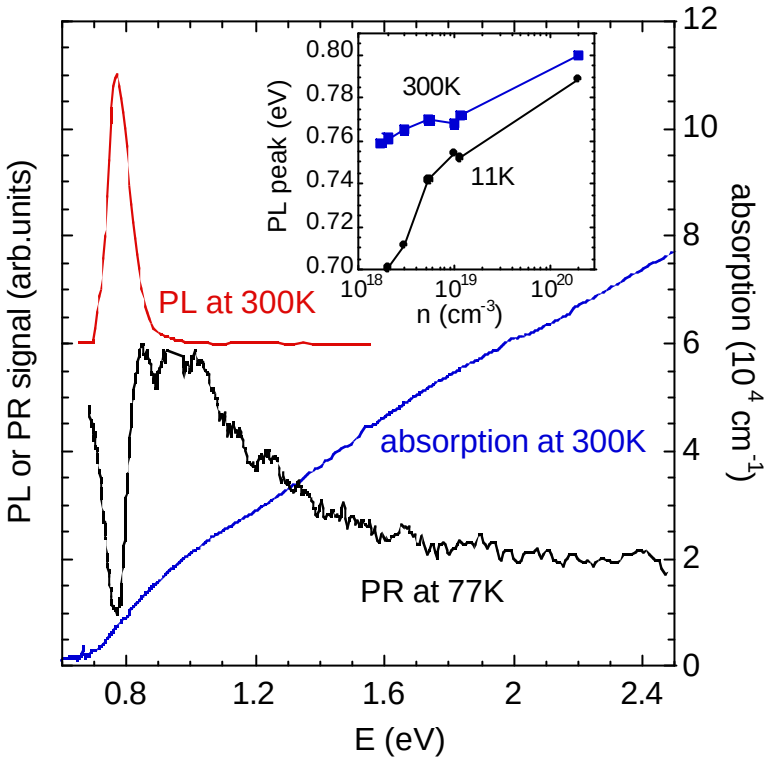

Figure 1. Optical absorption (300 K), PL (300 K), and PR (77 K) spectra of a typical InN sample. This sample is undoped with a room-temperature electron concentration of $5.48\times10^{18}cm^{-3}$. The inset shows the PL peak energy (300 K and 12 K) as a function of the free electron concentration.

Also, as shown in Fig. 1, the samples exhibit intense room temperature luminescence at energies close to the optical absorption edge. Finally, the 77 K PR spectrum exhibits a transition feature at 0.8 eV with a shape that is characteristic for direct gap interband transitions. As with the absorption spectrum, there is no discernible change in the PR signal near 2 eV. The simultaneous observations of the absorption edge, the PL and the PR features at essentially the same energy indicate that this energy position corresponds to the transition across the fundamental bandgap of InN.

The inset of Fig. 1 shows the peak energy of PL as a function of electron concentration obtained at room temperature and 11 K. The sample with the highest free electron concentration $n = 2\times10^{20}cm^{-3}$ is silicon doped. All the other samples are not intentionally doped. The samples with the lowest electron concentrations have mobilities m greater than 1000 cm^2/Vs. It is seen in the inset that the transition energies increase with increasing free electron concentration.

The temperature dependence of the PL peak energy can be also seen in the inset of Fig. 1. The PL peak energy decreases from 300 K to 11 K. The shift is smaller for samples with higher free electron concentration, ranging from 0.03 to 0.2 meV/K for samples under investigation. This behavior is in a stark contrast to the temperature dependence of the direct bandgap in most semiconductors, where typically a significant reduction of the bandgap is observed with increasing temperature [11].

More detailed studies of the temperature dependence of the PL were carried out on the sample with n=5.48×10^{18} cm^{-3} and m=615 cm^2/Vs. The results are shown in Fig. 2(a) and Fig. 2(b). As can be seen in Fig. 2(b), in addition to the small blueshift (nearly linear at ~ 0.1meV/K) of the PL peak energy, the integrated intensity of the PL decreases by ~ 20 times as the temperature is increased from 11 K to room temperature. The data in Fig.

2(a) also show a considerable increase of the linewidth of the PL spectra. The FWHM increases from 35 meV to 70 meV when the temperature increases from 11 K to room temperature. Therefore it can be concluded that there is no significant shift of the PL spectra, as the temperature induced line broadening can easily account for the observed small upward shift of the PL line maximum.

We have also measured the excitation power dependence of the PL. As shown in Fig. 3(a), the integrated PL intensity depends linearly on the excitation power over three orders of magnitude. The peak energy does not shift over this excitation power range. The linear dependence and the lack of any PL signal saturation effect again suggest that the PL originates from fundamental interband transitions in InN.

To further elucidate the nature of the observed PL emission, we have studied its hydrostatic pressure behavior. The PL peak energy as a function of applied pressure is shown in Fig. 3(b). The linear pressure coefficient is equal to 0.6 meV/kbar, which is considerably smaller than the pressure coefficient previously observed in other III-V compounds. For example, the pressure coefficient of GaN is 4.3 meV/kbar [12], $Al_xGa_{1-x}N$ is 4.1 meV/kbar for $0.12 < x < 0.6$ [13], and GaAs is 11 meV/kbar [14]. Using experimental elastic constants for sapphire and theoretical elastic constants for InN, we estimated the correction factor of the bandgap for coherently strained InN on sapphire to be 1.45. Therefore, the pressure dependence of the PL peak energy is between 0.6 meV/kbar and 0.9 meV/kbar. This unusually low pressure coefficient of InN is not totally unexpected since, as it has been shown previously, the pressure dependence of the energy gap of $In_xGa_{1-x}N$ alloys decreases rapidly with increasing In content [12, 15].

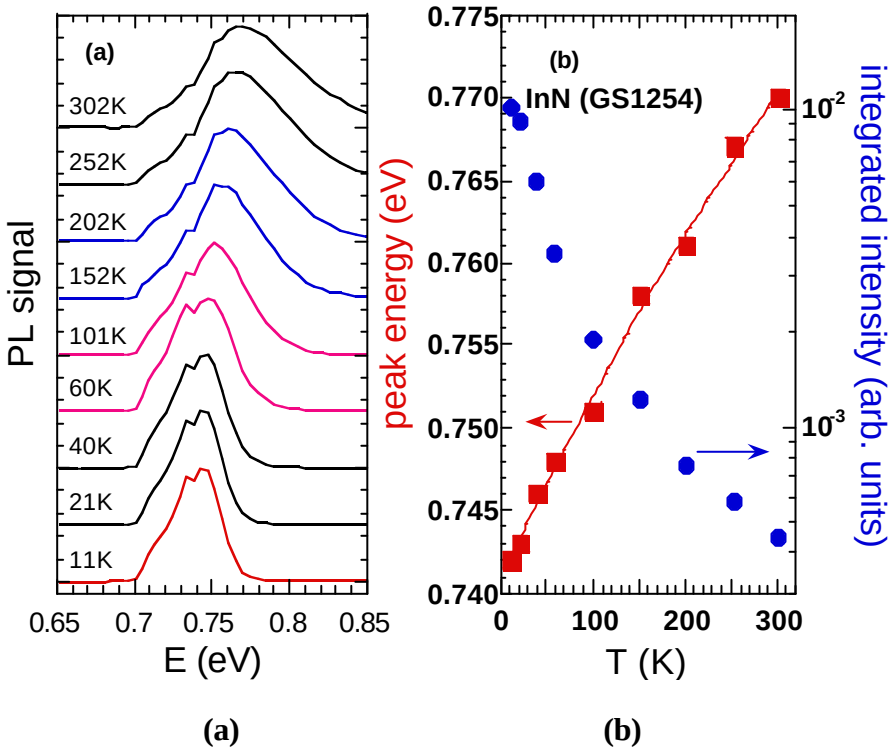

Figure 2. (a) PL spectra measured at different temperatures for the sample shown in Fig.1. The PL spectra are normalized to a constant peak height. (b) PL peak energy and PL integrated intensity (log scale) as a function of temperature. The line through the peak energy data serves as a guide to the eye.

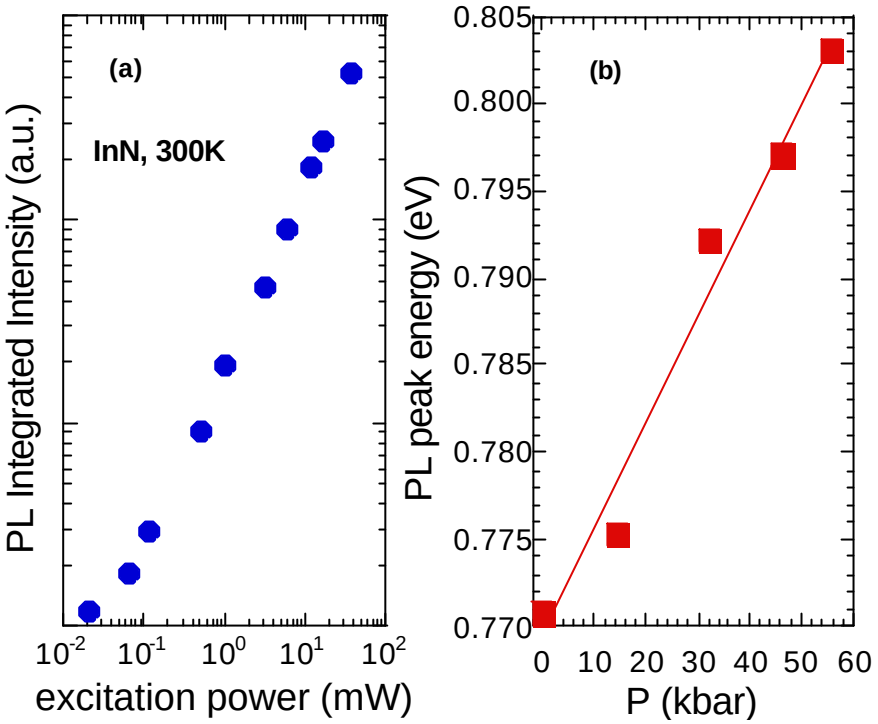

Figure 3. (a) The excitation power dependence of the room-temperature PL integrated intensity for the sample measured in Fig.1. (b) PL peak energy as a function of applied hydrostatic pressure.

The small pressure coefficient of the bandgap could partially explain the weak temperature dependence of the bandgap. The temperature coefficient of semiconductor bandgaps can be decomposed into two contributions, one originating in the change in the lattice constant due to thermal expansion, and the other one in the electron-phonon interaction [16]. The weak pressure dependence implies that there is only a very small contribution of the lattice expansion to the temperature induced bandgap change. Also, the small overall temperature coefficient implies that the electron-phonon coupling in this material may be also extraordinarily small.

4. Composition dependence of the band gap of $In_{1-x}Ga_xN$

InGaN alloys are under intense investigation because of their importance in applications in opto-electronic devices. The bandgap of 1.9 eV for InN has been frequently used as the end-point gap energy for extrapolating the composition dependence of their bandgaps [10]. The discovery of a narrow bandgap of InN is expected to have significant effects on the studies of InGaN.

The inset of Fig. 4 shows the room-temperature absorption (squared) curves for $In_{1-x}Ga_xN$ samples with a wide range of Ga compositions from 0 to 0.5. As expected, the absorption edge shows a strong blueshift from the bandgap of InN with increasing Ga content. The curves of absorption coefficient squared are essentially linear in the range of photon energy investigated, which also implies a direct fundamental bandgap. The observed slight non-linearity of the curves for small x can be attributed to the non-parabolicity of the conduction band resulting from the $\mathbf{k}\cdot\mathbf{p}$ interaction between the Γ_6-symmetry conduction band and the Γ_8-symmetry valence bands [17].

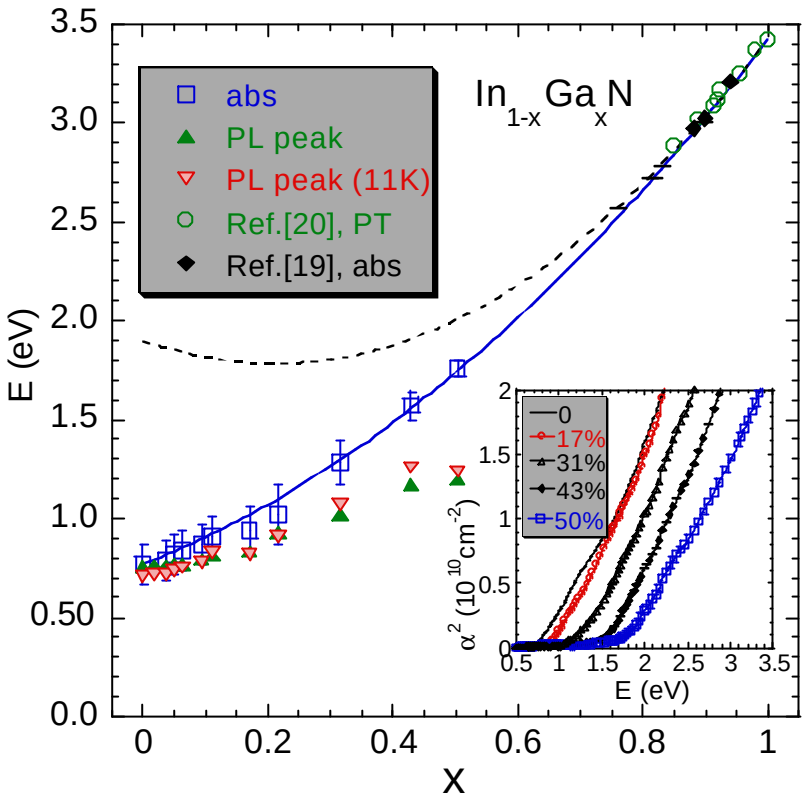

Figure 4. PL peak energy and bandgap determined by optical absorption as a function of composition. Some previously reported data on the Ga-rich side are also shown (Ref.[19] and [20]). All data are taken at room temperature unless otherwise noted. The solid curve shows the fit to the bandgap energies using a bowing parameter b = 1.43 eV. The dashed curve is the fit to the bandgap energies on the Ga-rich side assuming a bandgap of 1.9 eV for InN. Inset: Room-temperature absorption coefficient squared as a function of photon energy.

The bandgaps determined from the absorption edges in the inset are shown as a function of Ga concentration in Fig. 4. For Ga-rich $In_{1-x}Ga_xN$ alloys, numerous studies have been performed on the composition dependence of the band gap [18-21]. In order to see the composition dependence of the bandgap over the entire composition range, two sets of previously reported data on the Ga-rich side are also shown in Fig. 2. These bandgaps were measured by photomodulated transmission (PT) [20] and optical absorption [19], respectively. It can be seen that our data on the In-rich side makes a smooth transition to the data points on the Ga-rich side. This result further confirms that the absorption edge of InN observed near 0.77 eV indeed corresponds to the intrinsic fundamental bandgap of InN [7, 22]. As shown by the solid curve in Fig. 4 the composition dependence of the room-temperature bandgap over the entire composition range can be well fit by the following standard equation,

$$E_G(x) = 3.42\,x + 0.77\,(1-x) - 1.43\,x\,(1-x). \qquad \text{(in eV)} \qquad (1)$$

with a constant bowing parameter of b = 1.43 eV. This value of b is much smaller than previously reported bowing coefficients for which a bandgap of ~ 1.9 eV for InN was used as the lower-energy end point [18, 19], and is similar to that observed (1.3 eV) for the $Al_xGa_{1-x}N$ alloy system [13]. If an InN bandgap of 1.9 eV is assumed instead of 0.77 eV, for the two sets of data points on the Ga-rich side shown in Fig. 4, a bowing

coefficient as large as 2.63 eV is needed to accommodate the composition dependence on the Ga-rich side. This fit is shown as a dashed curve in Fig.4. It has been pointed out in Ref.[19] that the variety of experimental bandgaps on the Ga-rich side can be better fit with a pseudo-linear composition dependence. Our results show that this pseudo-linear composition dependence on the Ga-rich side is just the direct evidence of the small bowing over the entire composition range. An additional significance of Fig. 4 is that it demonstrates that the fundamental bandgap of this ternary alloy system alone covers a wide spectral region ranging from the near infrared at ~ 1.6 μm to the near ultra-violet at ~ 0.36 μm.

The composition dependence of the peak energy of the PL signal is also shown in Fig. 4. At higher Ga concentrations, the PL peak energy shifts towards lower energy as compared with the absorption edge. The observed Stokes shift increases with increasing Ga content and is as large as 0.56 eV for $x = 0.5$. The large, composition dependent Stokes shift indicates that the PL measurement is not a reliable technique to determine the bowing parameter. It also explains the origin of the much larger bowing parameter of 2.5 eV determined in recent PL studies of $In_{1-x}Ga_xN$ alloys [23].

5. Summary

In summary, we have studied the optical properties of InN and In-rich InGaN layers grown on sapphire by molecular-beam epitaxy. The bandgap energies of the InN films are found to lie between 0.7 and 0.8 eV, significantly below the values previously reported for InN. The PL peak energy has been measured as a function of the free electron concentration, temperature, laser excitation power, and hydrostatic pressure. We have also demonstrated that In-rich $In_{1-x}Ga_xN$ alloys with $x<0.5$ have small fundamental bandgap energies ranging from around 0.77 eV to 1.75 eV. The composition dependence of the bandgap can be well explained by a relatively small bowing parameter. The Stokes shift increases with increasing Ga concentration for the compositions investigated, suggesting spatial variation of the alloy composition and strong carrier localization in the samples.

The work at the Lawrence Berkeley National Laboratory is supported by the Director, Office of Science, Office of Basic Energy Sciences, Division of Materials Sciences and Engineering, of the U.S. Department of Energy under Contract No. DE-AC03-76SF00098. The work at Cornell University is supported by ONR Contract No. N000149910936

References

[1] Nakamura S and Fasol G 1997 Blue laser diode (Berlin: Springer)
[2] Tygai V A, Evstigneev A M, Krasiko A N, Andreeva A F, Malakhov V Ya 1977 Sov. Phys. Semicond. 11 1257
[3] Tansley T L and Foley C P 1986 J. Appl. Phys. 59 3241
[4] Guo Q and Yoshida A 1994 Jpn. J. Appl. Phys. 33 2453
[5] Look D C, Lu H, Schaff J, Jasinski J, Liliental-Weber Z 2002 Appl. Phys. Lett. 80 258
[6] Inushima T, Mamutin V V, Vekshin V A, Ivanov S V, Sakon T, Motokawa M, Ohoya S 2001 Crystal Growth 227-228 481
[7] Davydov V Yu, Klochikhin A A, Seisyan R P, Emtsev V V, Ivanov S V, Bechstedt F, Furthmüller J, Harima H, Mudryi A V, Aderhold J, Semchinova O, Graul J 2002 phys. stat. solidi (b) 229 R1

[8] Lu H, Schaff W J, Hwang J, Wu H, Yeo W, Pharkya A, Eastman L F 2000 Appl. Phys. Lett. 77 2548
[9] Sturge M D 1962 Phys. Rev. 127 768
[10] Wetzel C, Takeuchi T, Yamaguchi S, Katoh H, Amano H, Agasaki I 1998 Appl. Phys. Lett. 73 1994
[11] Shan W, Schmidt T J, Yang X H, Hwang S J, Song J J 1995 Appl. Phys. Lett. 66 985
[12] Shan W, Song J J, Feng Z C, Shurman M, Stall R A 1997 Appl. Phys. Lett. 71 2433
[13] Shan W, Ager III J W, Yu K M, Walukiewicz W, Haller E E, Martin M C, McKinney W R, Yang W 1999 J. Appl. Phys. 85 8505
[14] Wolford D J and Bradley J A 1985 Solid State Commun. 53 1069
[15] Perlin P, Gorczyca I, Suski T, Wisniewski P, Lepkowski S, Christensen N E, Svane A, Hansen M, DenBaars S P, Damiliano B, Grandjean N, Massies J 2001 Phys. Rev. B 64 115319
[16] Cohen M L and Chadi D J 1980 Semiconductor Handbook Balkanski M, ed. (Amsterdam: North Holland) Vol. 2 Chapter 4b
[17] Kane E O 1957 J. Phys. Chem. Solids 1 249
[18] O'Donnell K P, Martin R W, Trager-Cowan C, White M E, Esona K, Deatcher C, Middleton P G, Jacobs K, Van der Stricht W, Merlet C, Gil B, Vantomme A, Mosselmans J F W 2001 Mater. Sci. Eng. B 82 194
[19] Pereira S, Correia M R, Monteiro T, Pereira E, Alves E, Sequeira A D, Franco N 2001 Appl. Phys. Lett. 78 2137
[20] Shan W, Walukiewicz W, Haller E E, Little B D, Song J J, McCluskey M D, Johnson N M, Feng Z C, Schurman M, and Stall R A 1998 J. App. Phys. 84 4452
[21] O'Donnell K P, Martin R W, Pereira S, Bangura A, White M E, Van der Stricht W, Jacobs K 1999 phys. stat. sol. (b) 216 141
[22] Wu J, Walukiewicz W, Yu K M, Ager III J W, Haller E E, Lu H, Schaff W J, Saito Y, Nanishi Y 2002 Appl. Phys. Lett. 80 3967
[23] Davydov V Yu, Klochikhin A A, Emtsev V V, Ivanov S V, Vekshin V V, Bechstedt F, Furthmüller J, Harima H, Mudryi A V, Hashimoto A, Yamamoto A, Aderhold J, Graul J, Haller E E 2002 phys. stat. sol. (b) 230 R4